agriculture

MDPI

Article

Preparation and Characterization of Novel Magnesium Composite/Walnut Shells-Derived Biochar for As and P Sorption from Aqueous Solutions

Vladimír Frišták [1,*], Martin Pipíška [1], Vladimír Turčan [1], Stephen M. Bell [2], Haywood Dail Laughinghouse IV [3], Libor Ďuriška [4] and Gerhard Soja [5]

1 Department of Chemistry, Trnava University in Trnava, 91843 Trnava, Slovakia; martin.pipiska@truni.sk (M.P.); vladimir.turcan@tvu.sk (V.T.)
2 Institute of Environmental Science and Technology (ICTA-UAB), Universitat Autónoma de Barcelona, 08193 Barcelona, Spain; Stephen.Bell@uab.cat
3 Agronomy Department, Fort Lauderdale Research and Education Center, University of Florida-IFAS, Davie, FL 33314, USA; hlaughinghouse@ufl.edu
4 Institute of Materials Science, Faculty of Materials Science and Technology in Trnava, Slovak University of Technology in Bratislava, 91724 Trnava, Slovakia; libor.duriska@stuba.sk
5 Energy Department, Austrian Institute of Technology GmbH, 3430 Tulln, Austria; Gerhard.Soja@ait.ac.at
* Correspondence: fristak.vladimir.jr@gmail.com; Tel.: +421-33-592-1459

Citation: Frišták, V.; Pipíška, M.; Turčan, V.; Bell, S.M.; Laughinghouse, H.D., IV; Ďuriška, L.; Soja, G. Preparation and Characterization of Novel Magnesium Composite/Walnut Shells-Derived Biochar for As and P Sorption from Aqueous Solutions. *Agriculture* **2021**, *11*, 714. https://doi.org/10.3390/agriculture11080714

Academic Editors: Nguyen V. Hue and Bin Gao

Received: 21 June 2021
Accepted: 27 July 2021
Published: 28 July 2021

Abstract: Elevated or unnatural levels of arsenic (As) and phosphorus (P) concentrations in soils and waterbodies from anthropogenic sources can present significant hazards for both natural ecosystems and human food production. Effective, environmentally friendly, and inexpensive materials, such as biochar, are needed to reduce mobility and bioavailability of As and P. While biochar features several physicochemical properties that make it an ideal contaminant sorbent, certain modifications such as mineral-impregnation can improve sorption efficiencies for targeted compounds. Here, we conducted sorption experiments to investigate and quantify the potential utility of magnesium (Mg) for improving biochar sorption efficiency of P and As. We synthesized a Mg-modified walnut shells-derived biochar and characterized its ability to remove As and P from aqueous solutions, thereby mitigating losses of valuable P when needed while, at the same time, immobilizing hazardous As in ecosystems. SEM-EDX, FTIR and elemental analysis showed morphological and functional changes of biochar and the formation of new Mg-based composites (MgO, MgOHCl) responsible for improved sorption potential capacity by 10 times for As and 20 times for P. Sorption efficiency was attributed to improved AEC, higher SSA, chemical forms of sorbates and new sorption site formations. Synthetized Mg-composite/walnut shell-derived biochar also removed >90% of P from real samples of wastewater, indicating its potential suitability for contaminated waterbody remediation.

Keywords: biochar; phosphorus; arsenic; sorption; Mg-impregnation; chemical modification

1. Introduction

Although phosphorus (P) is crucial for crop growth, natural deposits of inorganic P are limited. Widespread application of P fertilizers and subsequent agricultural runoff has contaminated surface waterbodies, promoting eutrophication [1]. Phosphate concentrations as low as 20 µg/L can permit rapid growth of algae alongside oxygen depletion. The resulting harmful algal blooms produce toxins that diminish water fauna and flora populations [2].

As a chemical analog to P, arsenic (As) is a carcinogenic metalloid element toxic to human and wildlife cardiovascular, neurological and pulmonary systems [3]. Arsenic exists in organic (methyl arsenate and dimethyl arsenate) and inorganic (arsenite and arsenate) forms. Soil and water resources commonly suffer As contamination from industrial

activities, mining, smelting and intensive pesticide applications. The maximum As concentration allowed by the US EPA is 24 mg/kg for soil and 10 µg/L for drinking water [4]. Unfortunately, increased As concentrations in soil and water presents a significant hazard for flora, fauna, and human food production.

Effective, environmentally friendly, and inexpensive technologies are needed to reduce mobility and bioavailability of potential contaminants, such as As and P, in soils and waterbodies. Biochar in particular has received significant attention due to its nutrient sorption capacity and carbon sequestration benefits [5]. It is a stable, recalcitrant carbonaceous material that has shown promise in immobilizing a wide range of inorganic and organic substances in aquatic environments and soil matrices. Furthermore, our ability to manipulate biochar feedstocks (e.g., agricultural, industrial, kitchen wastes, and sludge) and production parameters (e.g., pyrolysis temperature, residence time, biomass pre-treatment, and product post-treatment) enables us to design biochars for specific environmental functions. The process of thermal decomposition in the partial or total absence of oxygen (i.e., pyrolysis) produces the highly porous structure biochar is known for, and the multiple associated beneficial properties (e.g., high surface area, abundant surface O-containing functional groups, improved cation exchange capacity, etc.). These characteristics are what make biochar such an promising tool for xenobiotic removal via processes such as physical adsorption, precipitation, electrostatic attraction, surface complexation, diffusion, and hydrogen bond formation [6].

However, the efficiency of biochar in water and soils can be compromised following the various biological, chemical, and physical interactions that inevitably occur in-situ. Oxidation of biochar in soil and its utilization as a carbon source by microorganisms and plant root systems can alter its structure and material properties [7]. Typical biochars derived from lignocellulose have limited oxoanionic sorption capacities [8]. Adsorption and immobilization capacities are mainly limited by the electrostatic repulsion force between unmodified biochar surfaces with negative charges and oxyanions, and low anion exchange capacity. In previous studies, we found negligible As and P anion sorption capacity of pure biochars in aqueous solutions [8,9].

The modification of biochars to overcome such limitations for soil and water remediation of inorganic contaminants, creating so-called "engineered or designer biochar", is now a commonly employed solution [10]. For instance, one possible way to prevent oxidation and ensure biochar effectiveness is the addition of minerals to the biochar, as described by Yang et al. [11]. Various studies have attempted to modify or synthesize new biochars with improved anionic sorption capacities [8,12,13]. In aqueous solutions, metal-impregnation is one of the most effective means of modifying biochars for improved inorganic sorption, especially for negatively charged oxyanions [14]. Commonly used metal salt solutions to impregnate biochar with metal-oxides include $MgCl_2$, $FeCl_3$, $Fe(NO_3)_3$ or $MnCl_2$ [14]. Following a soaking period, the biochar is removed from the solution and heated in normal atmospheric conditions featuring oxygen to complete the impregnation process.

Impregnation with $MgCl_2$ has received relatively little attention at present, however the few studies exploring its potential for the removal of oxyanions and metal cations have been promising. The use of $MgCl_2$ as an additive to biochar is attractive due to its easy hydrolysis and decomposition under higher temperatures. The key reactions (Equations (1)–(6)) that would occur during this process are the following [15]:

$$MgCl_2 \cdot 6H_2O \; 69\ ^\circ C \rightarrow MgCl_2 \cdot 4H_2O + 2H_2O \quad (1)$$

$$MgCl_2 \cdot 4H_2O \; 129\ ^\circ C \rightarrow MgCl_2 \cdot 2H_2O + 2H_2O \quad (2)$$

$$MgCl_2 \cdot 2H_2O \; 167\ ^\circ C \rightarrow aMgCl_2 \cdot nH_2O + bMgOHCl + bHCl + (2\text{-}na\text{-}b)H_2O \quad (1 \leq n \leq 2,\ a + b = 1) \quad (3)$$

$$MgCl_2 \cdot nH_2O \; 203\ ^\circ C \rightarrow Mg(OH)Cl \cdot 0.3H_2O + HCl + (n\text{-}1.3)H_2O \quad (1 \leq n \leq 2) \quad (4)$$

$$Mg(OH)Cl \cdot 0.3H_2O\ 235\ ^{\circ}C \rightarrow MgOHCl + 0.3H_2O \quad (5)$$

$$MgOHCl\ 415\ ^{\circ}C \rightarrow MgO + HCl \quad (6)$$

The hydrolysis and decomposition of $MgCl_2$ in pretreated biochar results in MgO, $Mg(OH)_2$ and Mg salts that alter its physicochemical properties and morphological characteristics. Afterall, the mineral fraction plays a relevant role in the stability and anionic sorption potential of biochar-based sorbents [16]. Zhang et al. [17] found that the final precipitated MgO comprised between approximately 8–20% of the content of the Mg-impregnated biochars of various feedstocks, which resulted in improved sorption of PO_4^{3-} and NO_{3-}. More recently, Jellali et al. [18] and Inyang et al. [19] demonstrated the significantly greater aqueous sorption capacities of Mg-impregnated biochars compared to un-modified controls for lead and phosphates, respectively. In the case of Pb, Mg-impregnated biochar was over seven times more efficient than the control [18].

Despite the promising results shown by Mg-impregnated biochars for removing and immobilizing inorganic contaminants, there remains a notable lack of in-depth studies dedicated to comprehensively investigating and quantifying the potential utility of this approach for As and P in aqueous solutions. In view of the chemical processes described and the necessity for inexpensive and effective options for contaminant remediation in real world settings (e.g., natural waterbodies polluted from excessive agricultural runoff), here we synthesized Mg-modified walnut shell-derived biochar to characterize its ability to remove As and P from both laboratory and field extracted (i.e., eutrophic lake water and byres wastewater) aqueous solutions. We expect greater sorption efficiencies to be displayed by the Mg-modified biochar, in comparison to the control, and our results are intended to provide insights into novel approaches for mitigating P losses in agroecosystems while at the same time immobilizing hazardous As.

2. Materials and Methods

2.1. Biochar Production and Chemical Modification

Commercially available walnut shell (WS) feedstock (AIT, Tulln) derived from food processing industry waste was twice washed in deionized water, oven-dried at 60 °C for 72 h, and sieved at a particle size of <2 mm. The obtained fraction was thermochemically converted into biochar via slow pyrolysis in a modified large-scale pyrolysis unit at 500 °C for 60 min (heating rate of 30 °C/min) under strict anoxic conditions (2L/min nitrogen flow). The produced pure biochar (BC) was homogenized, sieved, and the obtained fraction (0.5–1 mm) was stored in polypropylene boxes. The synthesis of magnesium composite/walnut shell-derived biochar (MgBC) was conducted according to Akgül et al. [20]. Briefly, 50 g of BC was mixed with 100 mL of 8% $MgCl_2$ at 150 rpm at a temperature of 22 °C for 4 h. Samples were then oven dried at 100 °C for 6 h and subsequently placed into a muffle oven for 3 h at 300 °C. The obtained MgBC was again sieved to produce uniform fractions (0.5–1 mm).

2.2. Physicochemical Characterization

The total carbon (C), hydrogen (H), and nitrogen (N) contents within the samples were analyzed by a CHNS-O Elemental Analyzer (CHNS-O EA 1108, Carlo Erba Instruments, Milano, Italy). The values of potential and active pH were determined after shaking the studied samples with deionized water or 0.1 mol/L KCl (ratio 1:15 m/v) for 60 min, followed by 60 min of stabilization. The values of electrical conductivity (EC) were determined in deionized water (1:10 m/v) after 24 h of material shaking. Anion exchange capacities (AEC) were determined by the bromide method according to Lawrinenko and Laird [21]. The concentration of functional groups was measured by Boehm titration [22]. The character and presence of surface functional groups were characterized by Fourier transform infrared spectroscopy (FTIR) (Perkin Elmer Spectrum System 2000, Shelton, CT, USA). Specific surface areas of the samples were quantified by the N_2 adsorption-de-sorption methodology (SORPTOMATIC 1990, Milano, Italy) followed by the Brunauer–Emmett–

Tellers (BET) model application. Total Mg concentrations were quantified by inductively coupled plasma mass spectrometry (ICP-MS) (Perkin Elmer, Elan DRCe 9000, Waltham, MA, USA) after decomposition with a digestion agent of HNO_3 and H_2O_2 [23]. The characterization experiments were conducted for each sample in 3 replicates. The morphological structures of BC and MgBC were captured through scanning electron microscopy (SEM) by the electron microscope JEOL JSM7600F (Tokyo, Japan) equipped with a field emission electron source (10 kV accelerating voltage and a beam current of 20 μA). Images were captured in a combined secondary and back-scattered electron regime, with a sample-to-detector distance of 10–15 mm.

2.3. Arsenic and Phosphorus Model Sorption Experiments

The sorption of As and P was evaluated via method under batch conditions according to OECD guideline no. 106, modified by Micháleková-Richveisová et al. [8] and Frišták et al. [9].

2.3.1. Effect of Contact Time

Kinetic experiments were carried out by suspending 0.25 g of sorbents in 7.5 mL of 60 mg/L PO_4^{3-} (prepared from 1 g/L PO_4^{3-} stock solution (KH_2PO_4) or 60 mg/L As (prepared from 1 g/L As stock solution (Na_2HAsO_4)) and shaken at 45 rpm (Orbital Shaker-Multi RS 60, Biosan) at a temperature of 22 ± 2 °C for the time periods of 5, 10, 60, 120, 240, 360, 1440, and 2880 min. The concentrations of unabsorbed PO_4^{3-} were determined by ion chromatography (IC, Dionex 1100 with conductivity detector ASRS 300, 4 mm) in aliquots after centrifugation (4000 min^{-1}, 5 min) and filtration using 0.45-μm syringe filters. Retention of PO_4^{3-} by the filters was tested before each use. The concentrations of unabsorbed As were determined by an electrochemical analyzer (SPC EcaFlow 150, electrochemical cell E353C and electrode E-T/Au, Istran) based on stripping chronopotentiometry.

Sorption of PO_4^{3-} and As were quantified according to the equation:

$$Q_{eq} = (C_0 - C_{eq}) \times V/w \quad (7)$$

where Q_{eq} is PO_4^{3-} or As uptake (mg/g), C_0 is the initial concentrations of PO_4^{3-} or As (mg/L) in liquid phase, C_{eq} is the equilibrium concentrations of PO_4^{3-} or As (mg/L) in liquid phase, V is the volume (L), and w is the amount of studied material (g).

2.3.2. Kinetic Models

For characterization of sorption kinetics, the empirical models of pseudo-1st, pseudo-2nd, and pseudo-*n*th orders were applied. The kinetic parameters were obtained by the software: MicroCal Origin 8.0 Professional (OriginLab Corporation, Northampton, MA, USA).

The pseudo-1st order model (Equation (8)) (Lagergren equation) can be defined as:

$$dQ_t/d_t = k_1 (Q_{eq} - Q_t) \quad (8)$$

where Q_{eq} represents the value of PO_4^{3-} or As sorbed at equilibrium time (mg/g), Q_t is the amount of PO_4^{3-} or As sorbed at time t (mg/g), and k_1 is the constant rate of pseudo-1st order action (1/min).

The pseudo-2nd order equation (Equation (9)) can be defined as:

$$dQ_t/d_t = k_2 (Q_{eq} - Q_t)^2 \quad (9)$$

where Q_t and Q_{eq} have equal importance as in the pseudo-1st order model and k_2 is the constant rate of the pseudo-2nd order (g/mg/min)

The pseudo-*n*th order (Equation (10)) can be defined as:

$$dQ_t/d_t = k_3 ({Q_{eq}}^n - {Q_t}^n)/Q^{n-1} \quad (10)$$

where n is the order of rate equation, Q_{eq} and Q_t have the same importance as in the pseudo-1st order, and k_3 represents the constant rate of the pseudo-nth order (g/mg min^{-1}).

2.3.3. Effect of Sorbate Initial Concentration

The equilibria of sorptions were studied in the range of 10–100 mg/L PO_4^{3-} or As at 22 ± 2 °C. Using 0.25 mg of biochar, 7.5 mL solution with varying concentrations of PO_4^{3-} and As were added. After shaking at 45 rpm at 22 ± 2 °C for 24 h, the materials were divided by centrifugation (4000 rpm, 5 min) and filtration. Amounts of residual PO_4^{3-} in the liquid phase were quantified by IC. Concentrations of As in the liquid phase were determined by SCP.

2.3.4. Applied Models of Adsorption Isotherms

For characterization of sorption data, the empirical equations of the models of Langmuir, Freundlich, and Sips (Langmuir–Freundlich) adsorption isotherms were applied. The adsorption isotherm parameters were obtained using non-linear regression via the software: MicroCal Origin 8.0 Professional (OriginLab Corporation, Northampton, MA, USA).

The model of Langmuir isotherm (Equation (11)) is given by the following empirical equation:

$$Q_{eq} = (bQ_{\max} C_{eq})/(1 + bC_{eq}) \quad (11)$$

where b represents the coefficient characterizing the affinity of material to sorbate ions in the matrix (L/mg), Q_{eq} is the amount of adsorbed sorbate at time of equilibrium (mg/g), C_{eq} is sorbate concentration in equilibrium (mg/L) and $Q_{\max}$ is the maximum sorption capacity at saturated sorbent binding sites (mg/g).

The Freundlich adsorption model (Equation (12)) is given by the following equation:

$$Q_{eq} = KC_{eq}^{(1/n)} \quad (12)$$

where n and K represent the Freundlich empirical constants characterizing intensity of sorption (L/g), C_{eq} is a sorbate concentration in equilibrium (mg/L) and Q_{eq} is the amount of sorbed ions at equilibrium (mg/g).

The combined form of Langmuir and Freundlich expressions (Equation (13)) (Sips isotherm) is given by the equation:

$$Q_{eq} = (Q_m(bC_{eq})^{1/n})/(1 + (bC_{eq})^{1/n}) \quad (13)$$

where Q_{eq} is the amount of sorbed sorbate at equilibrium (mg/g), b is the Sips constant characterizing sorbent affinity to sorbate ions in solution (L/mg), C_{eq} represents the sorbate equilibrium concentration in solution (mg/L), n is the index of heterogeneity and Q_m is the monolayer sorption capacity at saturated sorbent binding sites (mg/g).

2.4. Sorption of Phosphorus from Real Liquid Wastes

To determine the sorption capacity of the studied sorbents for phosphates under real conditions, 0.25 g of sorbents was mixed with 7.5 mL of real liquid samples (eutrophic lake water and byres wastewater after double filtration to remove macroscopic impurities) and shaken at 200 rpm at a temperature of 22 ± 2 °C for 24 h to reach sorption equilibrium. The concentrations of residual phosphates in samples were measured by IC after previous filtration and centrifugation (4000 rpm, 5 min).

3. Results and Discussion

3.1. Characterization of Pyrolysis Products

Physicochemical characterization of walnut shell biomass (WS), walnut shell-derived biochar (BC) and Mg-impregnated biochar (MgBC) revealed the effects of chemical activation via new magnesium composite synthesis on the final pyrolyzed products. The obtained results of ultimate and proximate analyses of the studied samples are listed in

Table 1. Strong deprotonation of binding sites and growth of ash content caused an increase in active and potential pH of BC and MgBC. Comparison of EC values showed the eminent effects of Mg-impregnation processes on the content of free or mobilizable inorganic ions. According to Table 1, the pyrolysis treatment of WS increased the anion exchange capacity from 0.53 cmol/kg to 1.39 cmol/kg in BC. Mg-impregnation multiplied AEC by almost 10 times compared to unimpregnated material.

Table 1. Basic physicochemical properties of studied materials (values are means ± SD). All measurement were taken in triplicates. SSA and total C, H, N are single measurement of analytically representative sample.

	WS	BC	MgBC
pH_{DW}	5.20 ± 0.04	7.61 ± 0.02	9.80 ± 0.03
pH_{KCl}	4.49 ± 0.00	6.74 ± 0.01	6.47 ± 0.03
EC (mS/cm)	0.23 ± 0.01	0.12 ± 0.01	0.81 ± 0.02
AEC (cmol/kg)	0.53 ± 0.02	1.39 ± 0.08	11.82 ± 0.19
SSA (m^2/g)	8.45	34.24	112.84
C (%)	49.10	82.92	64.15
H (%)	8.87	2.26	0.84
N (%)	0.01	0.02	0.01
Mg (mg/kg)	356 ± 6	705 ± 12	3250 ± 26
phenolic groups (mmol/g)	0.21 ± 0.02	0.50 ± 0.01	0.34 ± 0.01
lactonic groups (mmol/g)	0.36 ± 0.02	0.42 ± 0.01	0.30 ± 0.01
carboxylic groups (mmol/g)	0.45 ± 0.03	0.23 ± 0.01	ND *

* ND means not detected.

Determination of specific surface areas (SSA) of sorbents showed increases in the order of WS < BC < MgBC. Carbonization achieved during pyrolysis treatment raised the total C content from 49% for WS to 83% for BC. The carbon content was reduced by about 22% in MgBC. Removal of inorganic C during chemical modification and by the increase of Mg concentration explains the differences in total C content found in the materials before and after chemical modification. A similar trend was described by Chen et al. [5] and Micháleková-Richveisová [8].

The change in morphology of biomass and pyrolyzed materials was confirmed by SEM analysis with a magnification of 250 (Figure 1A–C). Micro-imaging of walnut shell-derived biochar before and after the Mg-impregnation process (Figure 1B,C) illustrates the partial filling of vacant micro- and mesopores by Mg-composites. Additionally, new surface composites were revealed. EDX mapping confirmed Mg localization in point composites of Mg (Figure 2). These coated forms are supposed to be oxide MgO and magnesium hydroxychloride (form MgOHCl). Akgül et al. [20] confirmed the formation of oxide forms of magnesium salts after Mg-chemical modification of tea waste-derived biochar.

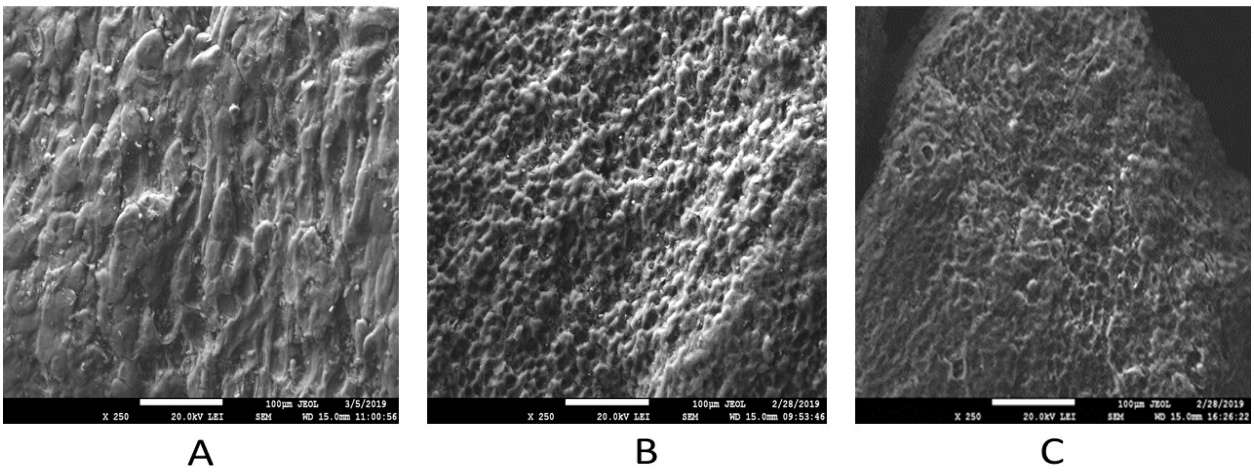

Figure 1. SEM (scanning electron microscopy) images of WS (**A**), BC (**B**) and MgBC (**C**) at magnification 250×.

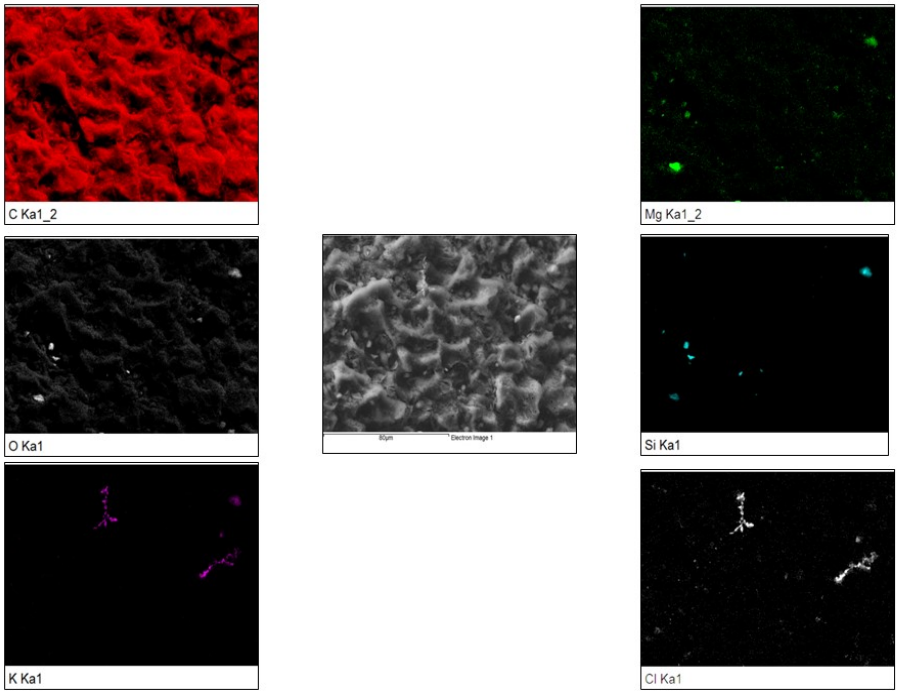

Figure 2. EDX (energy-dispersive X-ray spectroscopy) images of MgBC with selective mapping of carbon, oxygen, magnesium, silicon, chlorine and potassium.

Insight into physico-chemical properties of Mg-composite samples is key and mostly related to the functionality of material surfaces. Figure 3 shows comparisons of the ATR-FTIR spectra of WS-BC (A) and BC-MgBC (B) samples in the range 4000–400 cm^{-1}. Absorption peaks at 3600–3300 cm^{-1} are attributed to O–H vibration of moisture in the biomass of walnut shells [24]. Pyrolysis treatment, material carbonization and dehydration caused decreases in selected peak intensities. Additionally, the FTIR spectrum of BC materials reflects weaker intensities of absorption peaks at ν 1100–1250 cm^{-1} attributed to the stretching vibration of C–H, and ν 1050 cm^{-1} attributed to vibration of CO–H in primary hydroxyls compared to the WS spectrum. Analysis of the BC spectrum showed the presence of absorption peaks of C=C and C=O vibration at wavenumbers of 1500–1570 cm^{-1} that are typical for pyrolysis products. Comparison of BC and MgBC spectra revealed the changes in intensity of absorption peaks at ν 1680 cm^{-1} attributed to vibration of carboxylic C=O and 850 cm^{-1} to Mg–O–Mg. Therefore, these functional groups are potentially responsible for Mg binding from reaction solutions in the process of biochar chemical activation. Decreases in the concentration of surface carboxylic functional groups in MgBC were confirmed by Boehm titration as well (Table 1). Similar results were published by Micháleková-Richveisová [8] and Akgül et al. [20].

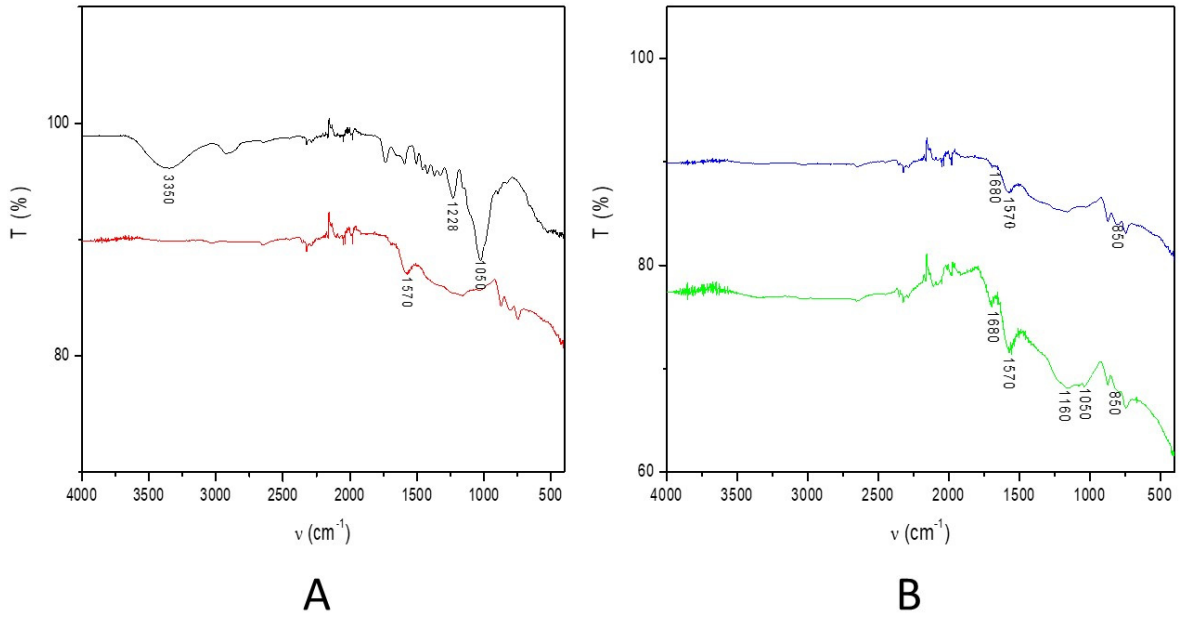

Figure 3. Comparison of ATR-FTIR spectra of WS (—) BC (—) (**A**) and BC (—) MgBC (—) (**B**) in the range of wavenumbers 4000–400 cm^{-1}.

3.2. Sorption Experiments

In aqueous solutions, phosphate and arsenate exist in several chemical species, with their concentrations controlled mainly by the pH value and the presence of other competitive chemicals [8,9]. At the studied pH_0 5.5–6, P exists predominantly in the forms of $H_2PO_4^-$ and HPO_4^{2-} [8]. Arsenic speciation at the studied pH value was mainly in the forms of $HAsO_4^{2-}$ and $H_2AsO_4^-$ [25]. Sorption of these anionic forms of phosphorus and arsenic from aqueous solutions represent a two-stage process (Figure 4A,B). The first step is characterized by rapid adsorption of sorbate within the first 360 min. After the saturation of free sorption sites on surfaces of BC and MgBC, there follows a second slower phase until equilibrium is achieved. Remenárová et al. [26] described this step as the slow diffusion of ions into pores and the formation of inner layer complexes. Sorption data showed negligible sorption of phosphates and arsenates by unmodified BC (Figure 4A,B), and thus a strong influence of surface repulsion between anions and negative surfaces [27].

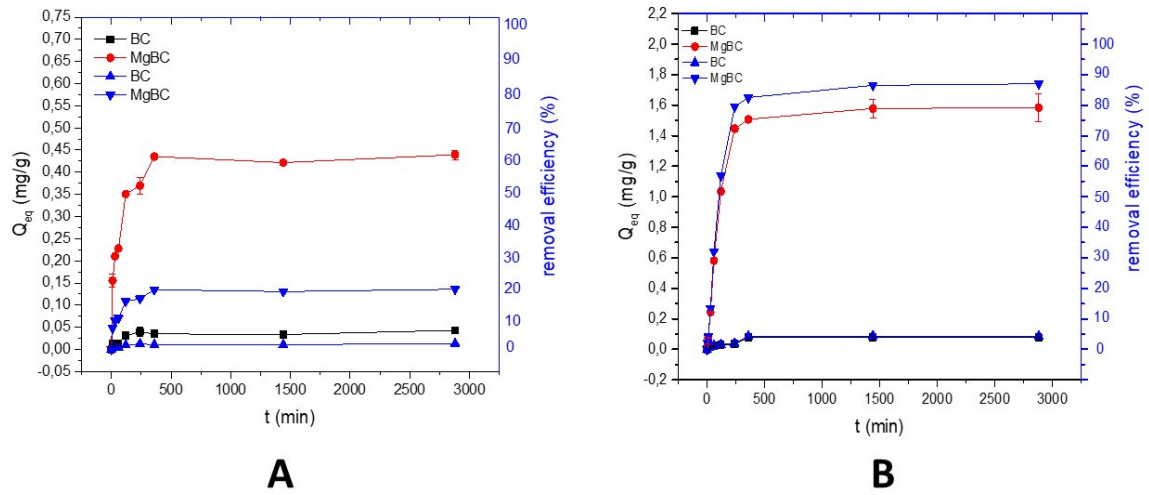

Figure 4. Effect of contact time on As (**A**) and P (**B**) sorption processes by walnut shell-derived biochar (BC), and Mg-impregnated walnut shell-derived biochar (MgBC). Experimental conditions: sorbent 33.3 g/L; initial concentration PO_4^{3-} 60 mg/L; initial concentration As 60 mg/L; pH_0 5.5-6; time periods 5, 10, 30, 60, 120, 240, 360, 1440, and 2880 min.

Chemical modification of biochar by synthesis of new Mg-composites showed significant positive effects on sorption capacities for both anionic sorbates. Sorption capacities of MgBC were higher by almost 20 times for phosphate and 10 times for arsenate. The obtained kinetic data were fitted and described by empirical models of pseudo-1st, pseudo-2nd and pseudo-nth order. Kinetic parameters calculated by the non-linear regression analysis are showed in Table 2. Coefficients of determination R^2 showed the greatest efficiency of the pseudo-nth order model for describing sorption kinetics of both P and As by BC and MgBC.

Table 2. Pseudo-1st, pseudo-2nd and pseudo-nth rate constants for sorption processes of P and As by sorbents based on BC and MgBC.

	Pseudo-First Order Rate Constants			Pseudo-Second Order Rate Constants			Pseudo-*n*th Order Rate Constants		
Sorbent	Q_{eq} [mg/g]	k_1 [1/min]	R^2	Q_{eq} [mg/g]	k_2 [g/mg/min]	R^2	Q_{eq} [mg/g]	k_n/n [g/mg/min]	R^2
				PO_4^{3-} Sorption					
BC	0.078	0.004	0.907	0.086	0.071	0.901	0.079	0.002/1.545	0.919
MgBC	1.607	0.008	0.994	1.754	0.006	0.971	1.572	0.017/0.683	0.999
				As Sorption					
BC	0.038	0.012	0.894	0.041	0.432	0.884	0.041	0.011/1.456	0.901
MgBC	0.416	0.019	0.924	0.439	0.068	0.960	0.436	0.002/2.050	0.991

The modelling of sorption equilibrium is crucial for better assessment of the sorption system. Sorption data of phosphate and arsenate obtained from equilibrium experiments showed adsorption isotherms of a conventional "L" shape (Figure 5). For the evaluation of P and As sorption equilibriums onto unmodified and modified walnut shell-derived biochar, the models of Langmuir, Freundlich and Sips adsorption isotherms were used. Model parameters obtained by non-linear regression analysis are listed in Table 3. The comparison of coefficients of determination showed the highest efficiency with the Sips model (combined Langmuir–Freundlich) compared to empirical conventional Langmuir and Freundlich models. Our previous works [9,25] confirmed the suitability of the Sips model for describing As sorption processes by chemically and physically activated biochars based on grape seeds and corn cob feedstocks. The values Q_{eq} of the Sips isotherm for phosphate were 0.110 mg/g (BC) and 1.810 mg/g (MgBC). Sorption data for arsenate showed values of Q_{eq} 0.008 mg/g (BC) and 1.083 mg/g (MgBC). Enhanced sorption capacities of Mg-modified biochar could be related to the main morphological changes and formations of magnesium composites in materials [28]. The values of SSA and AES correlate with obtained sorption data. Diverse sorption capacities for As and P can be discussed as different chemical sorption interactions of MgBC with chemical forms of P and As. We suppose that the main mechanism of As (III) sorption could be attributed to acid-based reactions and ligand exchanges. As (V) could be sorbed via electrostatic force. Mechanisms of phosphorus sorption processes can be characterized as a formation of stable phosphate precipitates on Mg-oxides.

Tables 4 and 5 show selected characteristics of modified pyrolysis materials with a focus on maximal sorption capacities for phosphate and arsenic. The presented values of maximal sorption capacities are calculated by a Langmuir model that may entail extrapolating the values out of an experimental concentration range. However, we found better results for P removal in comparison with Fe-modified orange peel-derived biochar (Table 4). In the case of As sorption, our synthesized material showed a higher sorption capacity as Mn-modified pinewood-derived biochar (Table 5).

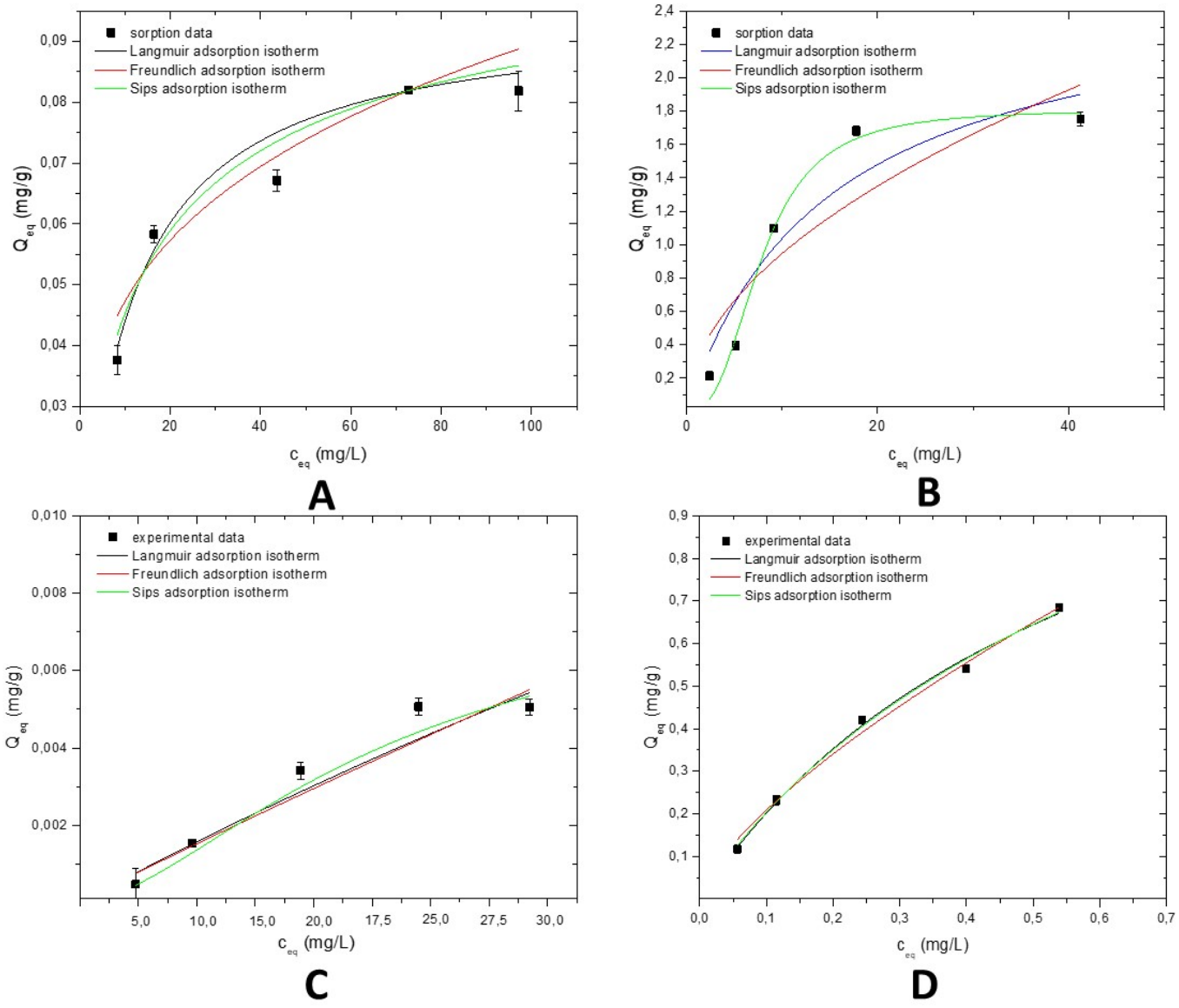

Figure 5. Equilibrium data of PO_4^{3-} (**A**,**B**) and As (**C**,**D**) sorption processes by walnut shell-derived biochar (**A**,**C**) and Mg-impregnated walnut shell-derived biochar (**B**,**D**) fitted by adsorption models of Langmuir, Freundlich and Sips isotherms. Experimental conditions: sorbent 33.3 g/L; C_0 PO_4^{3-} 10–100 mg/L; C_0 As 5–30 mg/L, pH_0 5.5–6; contact time 1440 min.

Table 3. Langmuir, Freundlich and Sips equilibrium parameters for PO_4^{3-} and As sorption by walnut shell-derived biochar (BC) and Mg-impregnated walnut shell-derived biochar (MgBC) obtained by non-linear regression analysis.

Sorbent	Adsorption Model/Parameter									
	Langmuir			Freundlich			Sips			
	Q_{max}(mg/g)	b	R^2	K	1/n	R^2	Q_m(mg/g)	K	n	R^2
					PO_4^{3-} sorption					
BC	0.095	0.087	0.963	0.025	0.277	0.960	0.110	0.134	0.716	0.967
MgBC	2.592	0.067	0.901	0.29012	0.513	0.856	1.810	0.004	2.716	0.987
					As sorption					
BC	0.039	0.209	0.934	0.007	0.954	0.932	0.008	2.924	1.665	0.896
MgBC	1.432	1.634	0.991	1.059	0.706	0.994	1.083	1.191	0.938	0.995

Table 4. Phosphate-sorption capacity (Q_{max}) of selected pyrolysis materials.

Sorbent	Feedstock	Pyrolysis Temperature (°C)	Modification Agent	Particle Size (mm)	Q_{max} (mg/g)	Reference
IBC A	corn cobs	500	$Fe(NO_3)_3$	0.5–1	1.99	[8]
IBC B	garden wood waste	500	$Fe(NO_3)_3$	0.5–1	2.75	[8]
IBC C	wood chips	500	$Fe(NO_3)_3$	0.5–1	3.2	[8]
MOP400	orange peel	400	$FeCl_2/FeCl_3$	<0.154	0.22	[29]
MOP700	orange peel	700	$FeCl_2/FeCl_3$	<0.154	1.24	[29]
FAC-B	carrot residue	400	$MgCl_2$ + cellulose acetate	<0.100	21.57	[30]
SSB-Mg	sewage sludge	500	$MgCl_2$	<0.250	28.1	[31]
MgBC	walnut shells	500	$MgCl_2$	0.5–1	2.59	this work

Table 5. Arsenic-sorption capacity (Q_{max}) of selected pyrolysis materials.

Sorbent	Feedstock	Pyrolysis Temperature (°C)	Modification Agent	Particle Size (mm)	Q_{max} (mg/g)	Reference
MgPM700	wood chips	700	$MgCl_2$	0.2–1	7.42	[25]
MgPM400	wood chips	400	$MgCl_2$	0.2–1	9.59	[25]
ZVI-RO	red oak	900	Fe_3O_4	<0.5	4.74	[32]
ZVI-SG	switchgrass	900	Fe_3O_4	<0.5	4.65	[32]
MPB	pine wood	600	$MnCl_2$	0.425–1	0.59	[33]
FBC	corn straw	600	$FeCl_3$	<0.3	6.80	[34]
NFMB	pine wood	600	$Ni(NO_3)_2$ + $FeCl_3$	0.425–1	4.38	[35]
MgBC	walnut shells	500	$MgCl_2$	0.5–1	1.43	this work

Additionally, the precise comparison should proceed with caution, as it is complicated to compare the sorption data due to the wide variety of experimental conditions (i.e., particle size, initial concentrations of sorbates, etc.).

Real eutrophic lake water and cow-byres wastewater was treated by BC and MgBC. Prior to the sorption separation experiment, the treated and filtered wastewater samples were characterized for determination of selected anions (Table 6). Removal of phosphate by BC from samples of eutrophic lake water was more effective in comparison to samples of cow-byres wastewater (Figure 6). Concentrations of competitive anions such as SO_4^{2-} and mainly Cl^- can play crucial roles in sorption mechanisms. On the other hand, MgBC showed promising sorption efficiency (more than 90%) in both real samples.

Table 6. Basic content of selected anions in real samples of eutrophic lake water and byres wastewater.

	pH	PO_4^{3-} (mg/L)	NO_3^- (mg/L)	SO_4^{2-} (mg/L)	Cl^- (mg/L)
eutrophic lake water	6.84 ± 0.08	1.56 ± 0.03	3.12 ± 0.08	4.05 ± 0.04	3.18 ± 0.12
byres wastewater	7.56 ± 0.12	14.45 ± 0.15	0.46 ± 0.01	247.8 ± 5.45	546.4 ± 5.11

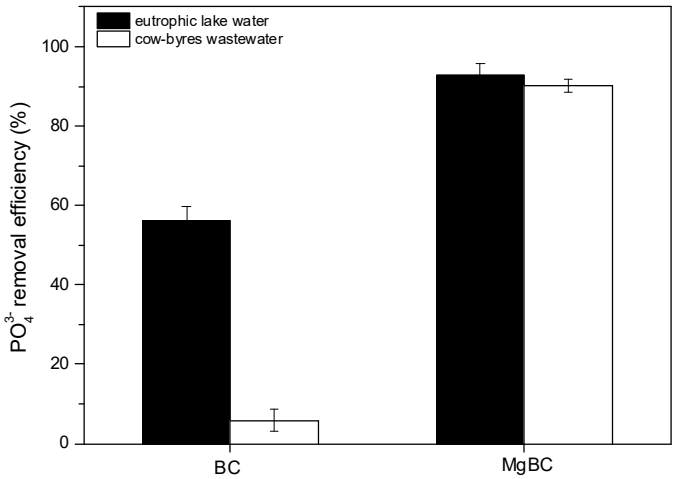

Figure 6. Phosphate removal capacity of BC and MgBC, from samples of eutrophic lake water and cow-byres wastewater. Experimental conditions: sorbent 33 g/L sorbent, 200 rpm, 22 ± 2 °C, 1440 min.

4. Conclusions

The chemical modification of walnut shell-derived biochar by magnesium and application of synthetized Mg-composited material in the sorption process of P and As from model aqueous solutions were presented. The process of Mg-impregnation provides an avenue to produce stable and effective sorbents for anionic chemical forms. The sorption process of As and P by BC and MgBC is a potentially fast process, with equilibrium reached within 360 min. The effect of Mg-modification caused significant morphological changes: new Mg-oxides creation and a significant increase of sorption capacity by 10 times for arsenic and 20 times for phosphorus. Removal efficiency was attributed to higher AEC, SSA and, mainly, the synthesis of new sorption sites of MgBC. Diverse sorption capacities for As and P can be attributed to different chemical sorption interactions of MgBC with chemical forms of P and As. The synthetized Mg-composite/walnut shell-derived biochar showed notable effectivity and potential under real-world conditions to remove phosphates from wastewaters, indicating its potential suitability as a tool for contaminated waterbody remediation.

Author Contributions: V.F., M.P., H.D.L.IV. designed and conceived sorption experiments, G.S. produced biochar sorbents, V.F., V.T., L.Ď. performed sorbent characterization experiments, V.F. and S.M.B. wrote the paper. All authors have read and agreed to the published version of the manuscript.

Funding: This research was funded by Scientific Grant Agency of the Ministry of Education, Science, Research, and Sport of the Slovak Republic, project number VEGA1/0178/20; and Trnava University in Trnava, project number 4/TU/2020.

Institutional Review Board Statement: Not applicable.

Informed Consent Statement: Not applicable.

Conflicts of Interest: The authors declare no conflict of interest. The funders had no role in the design of the study; in the collection, analyses, or interpretation of data; in the writing of the manuscript; or in the decision to publish the results.

References

1. Schindler, D.W.; Carpenter, S.; Chapra, S.C.; Hecky, R.E.; Orihel, D. Reducing Phosphorus to Curb Lake Eutrophication is a Success. *Environ. Sci. Technol.* **2016**, *50*, 8923–8929. [CrossRef]
2. Berthold, D.E.; Elazar, A.; Lefler, F.; Marble, C.; Laughinghouse, H.D., IV. Control of algal growth on greenhouse surfaces using commercial algaecides. *Sci. Agric.* **2021**, *78*, e20180292. [CrossRef]
3. Praveen, A.; Pandey, A.; Gupta, M. Nitric oxide alters nitrogen metabolism and PIN gene expressions by playing protective role in arsenic challenged *Brassica juncea* L. *Ecotoxicol. Environ. Saf.* **2019**, *176*, 95–107. [CrossRef]
4. Kumar, A.; Bhattacharya, T. Removal of Arsenic by Wheat Straw Biochar from Soil. *Bull. Environ. Contam. Toxicol.* **2021**, *9*, 1–8. [CrossRef]
5. Chen, Q.; Qin, J.; Cheng, Z.; Huang, L.; Sun, P.; Chen, L.; Shen, G. Synthesis of a stable magnesium-impregnated biochar and its reduction of phosphorus leaching from soil. *Chemosphere* **2018**, *199*, 402–408. [CrossRef] [PubMed]
6. Frišták, V.; Pipíška, M.; Lesný, J.; Soja, G.; Friesl-Hanl, W.; Packová, A. Utilization of biochar sorbents for Cd^{2+}, Zn^{2+} and Cu^{2+} ions separation from aqueous solutions: Comparative study. *Environ. Monit. Assess.* **2015**, *187*, 4093. [CrossRef]
7. Zimmermann, A.R. Abiotic and microbial oxidation of laboratory-produced black carbon (Biochar). *Environ. Sci. Technol.* **2010**, *44*, 1295–1301. [CrossRef] [PubMed]
8. Micháleková-Richveisová, B.; Frišták, V.; Pipíška, M.; Duriska, L.; Moreno-Jiménez, E.; Soja, G. Iron-impregnated biochars as effective phosphate sorption materials. *Environ. Sci. Pollut. Res.* **2016**, *24*, 463–475. [CrossRef]
9. Frišták, V.; Micháleková-Richveisová, B.; Víglašová, E.; Ďuriška, L.; Galamboš, M.; Moreno-Jimenéz, E.; Pipíška, M.; Soja, G. Sorption separation of Eu and as from single-component systems by Fe-modified biochar: Kinetic and equilibrium study. *J. Iran. Chem. Soc.* **2017**, *14*, 521–530. [CrossRef]
10. Rajapaksha, A.U.; Chen, S.; Tsang, D.C.; Zhang, M.; Vithanage, M.; Mandal, S.; Gao, B.; Bolan, N.; Ok, Y.S. Engineered/designer biochar for contaminant removal/immobilization from soil and water: Potential and implication of biochar modification. *Chemosphere* **2016**, *148*, 276–291. [CrossRef] [PubMed]
11. Yang, F.; Zhao, L.; Gao, B.; Xu, X.; Cao, X. The Interfacial Behavior between Biochar and Soil Minerals and Its Effect on Biochar Stability. *Environ. Sci. Technol.* **2016**, *50*, 2264–2271. [CrossRef]
12. Fristak, V.; Pipíška, M.; Soja, G. Pyrolysis treatment of sewage sludge: A promising way to produce phosphorus fertilizer. *J. Clean. Prod.* **2018**, *172*, 1772–1778. [CrossRef]

13. Gao, X.; Peng, Y.; Guo, L.; Wang, Q.; Guan, C.Y.; Yang, F.; Chen, Q. Arsenic adsorption on layered double hydroxides biochars and their amended red and calcareous soils. *J. Environ. Manag.* **2020**, *271*, 111045. [CrossRef]
14. Sizmur, T.; Fresno, T.; Akgül, G.; Frost, H.; Moreno-Jiménez, E. Biochar modification to enhance sorption of inorganics from water. *Bioresour. Technol.* **2017**, *246*, 34–47. [CrossRef] [PubMed]
15. Huang, Q.; Lu, G.; Wang, J.; Yu, J. Thermal decomposition mechanisms of $MgCl_2$ $6H_2O$ and $MgCl_2$ H_2O. *J. Anal. Appl. Pyrolysis.* **2011**, *91*, 159–164. [CrossRef]
16. Xie, Y.; Helvenston, E.M.; Shuller-Nickles, L.C.; Powell, B.A. Surface complexatin modeling of Eu(III) and U(VI) interactions with graphene oxide. *Environ. Sci. Technol.* **2016**, *50*, 1821–1827. [CrossRef]
17. Zhang, M.; Gao, B.; Yao, Y.; Xue, Y.; Inyang, M. Synthesis of porous MgO-biochar nanocomposites for removal of phosphate and nitrate from aqueous solutions. *Chem. Eng. J.* **2012**, *210*, 26–32. [CrossRef]
18. Jellali, S.; Diamantopoulos, E.; Haddad, K.; Anane, M.; Durner, W.; Mlayah, A. Lead removal from aqueous solutions by raw sawdust and magnesium pretreated biochar: Experimental investigations and numerical modelling. *J. Environ. Manag.* **2016**, *180*, 439–449. [CrossRef]
19. Inyang, M.I.; Gao, B.; Yao, Y.; Xue, Y.; Zimmerman, A.; Mosa, A.; Pullammanappallil, P.; Ok, Y.S.; Cao, X. A review of biochar as a low-cost adsorbent for aqueous heavy metal removal. *Crit. Rev. Environ. Sci. Technol.* **2015**, *46*, 406–433. [CrossRef]
20. Akgül, G.; Maden, T.B.; Diaz, E.; Moreno-Jiménez, E. Modification of tea biochar with Mg, Fe, Mn and al salts for efficient sorption of PO_4^{3-} and Cd^{2+} from aqueous solutions. *J. Water Reuse Desal.* **2019**, *9*, 57–66. [CrossRef]
21. Lawrinenko, M.; Laird, D.A. Anion exchange capacity of biochar. *Green Chem.* **2015**, *17*, 4628–4636. [CrossRef]
22. Goertzen, S.L.; Thériault, K.D.; Oickle, A.M.; Tarasuk, A.C.; Andreas, H.A. Standardization of the boehm titration. Part I. CO_2 expulsion and endpoint determination. *Carbon* **2010**, *48*, 1252–1261. [CrossRef]
23. Enders, A.; Lehmann, J. Comparison of wet-digestion and dry-ashing methodsfor total elemental analysis of biochar. *Commun. Soil Sci. Plant Anal.* **2012**, *43*, 1042–1052. [CrossRef]
24. De la Rosa, J.M.; Paneque, M.; Miller, A.Z.; Knicker, H. Relating physical and chemical properties of four different bio-chars and their application rate to biomass production of Lolium perenne on a Calcic Cambisol during a pot experiment of 79 days. *Sci. Total Environ.* **2014**, *499*, 175–184. [CrossRef]
25. Frišták, V.; Moreno-Jiménez, E.; Bucheli, T.D.; Fančovičová, J.; Soja, G.; Schmidt, H.P. Engineered pyrogenic materials as tools to affect arsenic mobility in old mine site soil of Mediterranean region. B. *Environ. Contam. Toxic.* **2020**, *2*, 265–272. [CrossRef]
26. Remenárová, L.; Pipíška, M.; Florková, E.; Horník, M.; Rozložník, M.; Augustín, J. Zeolites from coal fly ash as efficient sorbents for cadmium ions. *Clean. Technol. Environ.* **2014**, *16*, 1551–1564. [CrossRef]
27. Janus, A.; Pelfréne, A.; Heymans, S.; DeboffeCh, D.F.; Waterlot, C. Elaboration, characteristics and advantages of biochars for the management of contaminated soils with a specific overview on miscanthus biochars. *J. Environ. Manag.* **2015**, *162*, 275–289. [CrossRef]
28. Víglašová, E.; Galamboš, M.; Danková, Z.; Krivosudský, L.; Lengauer, C.L.; Hood-Nowotny, R.; Soja, G.; Rompel, A.; Matík, M.; Briančin, J. Production, characterization and adsorption studies of bamboo-based biochar/montmorillonite composite for nitrate removal. *Waste Manag.* **2018**, *79*, 385–394. [CrossRef]
29. Chen, B.; Chen, Z.; Li, S. A novel magnetic biochar efficiently sorbs organic pollutants and phosphate. *Bioresour. Technol.* **2011**, *102*, 716–723. [CrossRef]
30. Pinto, M.C.E.; da Silva, D.D.; Gomes, A.L.A.; Leite, V.S.A.; Moraes, A.R.F.; Novais, R.F.; Tronto, J.; Pinto, F.G. Film based on magnesium impregnated biochar/cellulose acetate for phosphorus adsorption from agueous solution. *RSC Adv.* **2019**, *9*, 5620–5627. [CrossRef]
31. Nardis, B.O.; Carneiro, J.S.S.; Souza, I.M.G.; Barros, R.G.; Melo, L.C.A. Phosphorus recovery using magnesium-enriched biochar and its potential use as fertilizer. *Arch. Agron. Soil. Sci.* **2021**, *67*, 1017–1033. [CrossRef]
32. Bakshi, S.; Banik, C.; Rathke, S.; Laird, D.A. Arsenic sorption on zero-valent iron-biochar complexes. *Water Res.* **2018**, *137*, 153–163. [CrossRef]
33. Wang, S.; Gao, B.; Li, Y.; Mosa, A.; Zimmerman, A.R.; Ma, L.Q.; Harris, W.G.; Migliaccio, K.W. Manganese oxide-modified biochars: Preparation, characterization, and sorption of arsenate and lead. *Bioresour. Technol.* **2015**, *181*, 13–17. [CrossRef] [PubMed]
34. He, R.; Peng, Z.; Lyu, H.; Huang, H.; Nan, Q.; Tang, J. Synthesis and characterization of an iron-impregnated biochar for aqueous arsenic removal. *Sci. Total Environ.* **2018**, *612*, 1177–1186. [CrossRef]
35. Wang, S.; Gao, B.; Li, Y.; Zimmerman, A.R.; Cao, X. Sorption of arsenic onto Ni/Fe layered double hydroxide (LDH)-biochar composites. *RSC Adv.* **2016**, *6*, 17792. [CrossRef]